Disturbance attenuation–based sliding mode control with disturbance observer for mismatched uncertain system

Jianguo Guo, Yuchao Liu, Cheng Cheng and Jun Zhou

Abstract

A disturbance attenuation–based sliding mode control approach with an extended disturbance observer is proposed for systems with mismatched uncertainties. A novel adaptive sliding surface consisting of the disturbance estimation is presented to eliminate the effect of mismatched disturbance in the sliding mode. The proposed method exhibits the following two attractive features. First, the asymptotical stability of adaptive sliding mode can be guaranteed even if the disturbance estimation error of the disturbance observer exists. Second, the nominal performance of the proposed approach is close to that of the traditional sliding mode control method in the absence of uncertainties. Finally, simulation results of the numerical and application examples show that the proposed nonlinear sliding mode control approach has the better dynamic performance as well as robustness and chattering reduction compared with other nonlinear sliding mode control methods.

Keywords

Sliding mode control, mismatched uncertainties, chattering reduction, disturbance observer, robustness

Introduction

It is well known that sliding mode control (SMC) is robust to matched uncertainties since it has the property of invariance on the sliding mode in the presence of matched uncertainties and disturbances. SMC method as an effective and popular control strategy has been widely used in diverse fields in order to obtain satisfactory performance.[1,2] However, uncertainties existing in control systems may not necessarily satisfy the matching criteria, examples can be seen in a lot of practical systems such as permanent magnet synchronous motors,[3,4] MAGnetic LEVitation (MAGLEV) suspension system,[5] flexible joint manipulator,[6] and control system for missiles.[7,8] When the system is subjected to unmatched uncertainty, invariance and robustness with traditional SMC would fail due to the fact that SMC is not satisfied with matching condition.

In order to eliminate the effect, the mismatched uncertainties in practical applications, many authors are committed to researching activities to address the problem of mismatched uncertainty in SMC. In general, these methods can be divided into the following two categories.

The first category mainly uses different control strategies to reduce the impact of mismatched uncertainties on the stability of the system, such as linear matrix

Institute of Precision Guidance and Control, School of Astronautics, Northwestern Polytechnical University, Xi'an, China

Corresponding author:
Yuchao Liu, Institute of Precision Guidance and Control, School of Astronautics, Northwestern Polytechnical University, Xi'an 710072, China.
Email: lyc-me@qq.com

inequality (LMI)-based approach,[9] the Riccati approach,[10] fuzzy and neural network based control,[11–13] adaptive approach,[14–17] invariant ellipsoid method,[18] and integral SMC approach.[19–22] The uncertainty of the mismatch uncertainties requires the bounds or vanity of the H2 norm in above methods. However, it is not a reasonable assumption of the actual system. For example, lumped uncertainties may have nonzero steady-state values, and there are no bounded H2 norms.[23,24]

The second category to address the problem of mismatched uncertain systems is usually use the method composed of the backstepping and SMC method.[25,26] The key idea of these approaches is based on a virtual control method in frame of the backstepping approach and the state to reach the surface and slide to the desired equilibrium using the SMC method. SMC method plays an important role in these methods. It is an effective control method that the traditional sliding mode with the disturbance observer (DO) for mismatched nonlinear systems.[27,28] The approach can reduce the effect of the mismatched uncertainties by employing the disturbance estimation of DO. However, the dynamic performance in the sliding mode is seriously subject to the estimation error of the mismatch uncertainties.

In this article, a new approach is proposed based on the second category method, and the main contributions are listed as follows:

1. The adaptive sliding surface with DO is proposed in order that the sliding motion of SMC is insensitive to the mismatched disturbance.
2. The effect of estimation error associated with mismatched uncertainties can be eliminated so as to guarantee the asymptotical stability of system.
3. The sliding surface can be designed when the initial states are unknown.
4. The control with adaptive term is modified to alleviate the chattering problem further. The proposed approach can be implemented when the bound on the estimation of uncertainty is not known exactly.

The remaining part of the article is organized as follows: the problem and objective are stated in section "Problem formulation." The control approach consisting of a novel adaptive sliding surface with DO is described. The stability is analyzed in section "Disturbance attenuation–based SMC method." The performance is illustrated by simulation examples in section "Numerical example." Finally, conclusions are reported in section "Conclusion."

Problem formulation

Consider the following system

$$
\begin{aligned}
\dot{x}_1 &= x_2 + d(t) \\
\dot{x}_2 &= a(x) + b(x)u \\
y &= x_1
\end{aligned}
\tag{1}
$$

where x_1 and x_2 are the states, u is the control input, $d(t)$ is the unmeasurable disturbance, y is the output, and $b(x) \neq 0$.

Assumption 1. The disturbance in system (1) is bounded and defined by $d^* = \sup_{t>0} |d(t)|$.

Assumption 2. The disturbance in system (1) is continuous and satisfies

$$
\left| \frac{d^j d(t)}{dt^j} \right| \leq \mu \quad j = 0, 1, 2, \ldots, r
\tag{2}
$$

where μ is a positive number.

Remark 1. The class of disturbance in Assumption 2 is much larger than the disturbance in Assumption 1. It may be noted that the disturbance in Assumption 2 is not required to know the bound μ.

The objective is to design control u so that the system output is not affected by the mismatched uncertainty $d(t)$.

SMC with DO

The sliding mode surface for system (1) affected by the mismatched disturbance is designed as follows[5]

$$
\sigma = x_2 + cx_1 + \hat{d}
\tag{3}
$$

where $c > 0$ is a control parameter to be designed and $\hat{d}$ is the disturbance estimate of $d(t)$. Then, DO can be written as follows[5]

$$
\begin{aligned}
\dot{p} &= -lg_2 p - l[g_2 lx + f(x) + g_1(x)u] \\
\hat{d} &= p + lx
\end{aligned}
\tag{4}
$$

where $f(x) = [x_2 \ a(x)]^T$, $x = [x_1 \ x_2]^T$, $g_1(x) = [0 \ b(x)]^T$, $g_2 = [1 \ 0]^T$, and $\hat{d}$, p, and l are the estimations of the disturbance $d(t)$, the internal state of nonlinear observer (4), and the observer gain to be designed when $lg_2 > 0$ holds, respectively.

Accordingly, the SMC law is designed as follows[5]

$$
u = -b^{-1}(x)\left[a(x) + c\left(x_2 + \hat{d}\right) + ksgn(\sigma) \right]
\tag{5}
$$

Combining equations (1), (3), (4), and (5) leads to

$$\dot{\sigma} = -ksgn(\sigma) + (c + lg_2)\left(d - \hat{d}\right) \quad (6)$$

According to equation (6), the states in system (1), which stay initially outside the sliding surface, will reach the sliding surface $\sigma = 0$ in finite time when the switch gain in the control law (equation (5)) satisfies $k > (c + lg_2)(d - \hat{d})$.

When $\sigma = 0$, the sliding motion in equation (3) is obtained as follows

$$\dot{x}_1 = -cx_1 + d - \hat{d} \quad (7)$$

Remark 2. The state in equation (7) cannot be driven to the desired equilibrium point asymptotically based on the sliding mode control with disturbance observer (DO-SMC) law (equation (5)) when the derivation of the disturbance $d(t)$ is bounded and satisfies $\lim_{t \to \infty} \dot{d}(t) \neq 0$. As a consequence, the DO-SMC (equation (4)) is sensitive to estimation error of the mismatched disturbance.

Extended DO-modified SMC

The modified sliding mode surface for system (1) affected by the mismatched disturbance is designed as follows[6]

$$\sigma^* = \sigma - \sigma(0)e^{-\alpha t} \quad (8)$$

where σ is given in equation (3) and α is a positive constant. The extended DO can be defined as follows[6]

$$
\begin{aligned}
\hat{d} &= p_{11} + l_{11}x_1 \\
\dot{p}_{11} &= -l_{11}\left(x_2 + \hat{d}\right) + \dot{\hat{d}} \\
\dot{\hat{d}} &= p_{12} + l_{12}x_1 \\
\dot{p}_{12} &= -l_{12}\left(x_2 + \hat{d}\right)
\end{aligned}
\quad (9)
$$

where $\hat{d}$ and $\dot{\hat{d}}$ are the estimators of the disturbances $d(t)$ and $\dot{d}(t)$, respectively, p_{11} and p_{12} are auxiliary variables, and l_{11} and l_{12} are positive constants. The estimation error of the extended DO is bound by $||e_d|| \leq \lambda$, where $e_d = [d - \hat{d}, \dot{d} - \dot{\hat{d}}]^T$, $\lambda > 0$ is relative with μ.[6]

The extended disturbance observer–modified sliding mode control (EDO-MSMC) law is designed as follows[6]

$$
\begin{aligned}
u = &-b^{-1}(x) \\
&\left[a(x) + c\left(x_2 + \hat{d}\right) + \alpha\sigma(0)e^{-\alpha t} + k_l\sigma^* + k_s sgn(\sigma^*)\right]
\end{aligned}
\quad (10)
$$

Similarly, combining equations (1), (8), and (10) leads to

$$\dot{\sigma}^* = -k_l\sigma^* - k_s sgn(\sigma^*) + c\left(d - \hat{d}\right) + \dot{\hat{d}} \quad (11)$$

where $k_l > 0$ and $k_s > |c(d - \hat{d}) + \dot{\hat{d}}|$.

When $\sigma^* = 0$ in equation (8), the sliding motion can be obtained as follows

$$\dot{x}_1 = -cx_1 + d - \hat{d} + \sigma(0)e^{-\alpha t} \quad (12)$$

Remark 3. EDO-MSMC can be obtained when the initial state of system is known. In addition, the state x_1 is not asymptotically stable and $||x_1|| \leq \lambda$, where λ depends on the estimation error. It is noted that the estimation error of mismatched uncertainties will influence the stability of the state x_1 and the effect of chattering on the sliding mode cannot be totally eliminated in the above approaches; thus, the novel adaptive sliding surface with extended DO is proposed to improve the dynamical performance.

Disturbance attenuation–based SMC method

Adaptive SMC with extended DO

The novel adaptive sliding surface with extended DO (equation (9)) for system (1) is designed as follows

$$\bar{\sigma} = x_2 + \frac{cx_1}{|x_1| + k^2 e^{-\beta t}} + \hat{d} \quad (13)$$

where $\dot{k} = -(c\gamma|x_1|ke^{-\beta t}/(|x_1| + k^2 e^{-\beta t})) - \gamma k$, $k(0) > 0$, $\gamma > 0$, and $\beta > 0$.

Stability of sliding mode dynamics

When the designed sliding surface $\bar{\sigma} = 0$, it can be obtained as

$$\dot{x}_1 = -\frac{cx_1}{|x_1| + k^2 e^{-\beta t}} + d - \hat{d} \quad (14)$$

The other candidate Lyapunov function is as follows

$$V(x_1, k) = \frac{x_1^2}{2} + \frac{k^2}{2\gamma} \quad (15)$$

Accordingly, the derivative of $V(x_1, k)$ in equation (15) is

$$\dot{V}(x_1, k) = -\frac{cx_1^2}{|x_1| + k^2 e^{-\beta t}} + \left(d - \hat{d}\right)x_1 + \frac{k\dot{k}}{\gamma} \quad (16)$$

Using adaptive parameter $\dot{k}$ into equation (16) yields

$$\begin{aligned}
\dot{V}(x_1, k) &= -c|x_1| + \left(d - \hat{d}\right)|x_1| - k^2 \\
&\leq -c|x_1| + |d - \hat{d}||x_1| - k^2 \\
&= -\left(c - |d - \hat{d}|\right)|x_1| - k^2 \\
&\leq -(c - \lambda)|x_1| - k^2
\end{aligned} \qquad (17)$$

When $c > \lambda$, it can be verified that the sliding surface (17) is exponentially stable according to Lyapunov stability theory.

Stability of SMC

Theorem 1. Suppose that Assumption 2 holds for system (1) and the sliding mode is chosen as equation (13), the closed-loop system is asymptotically stable when the control law is designed as

$$\begin{aligned}
u = -b^{-1}(x) &\left[a(x) + \frac{cke^{-\beta t}\left(x_2 k + k\hat{d} - 2x_1\dot{k} + x_1 k\beta\right)}{\left(|x_1| + k^2 e^{-\beta t}\right)^2} \right. \\
&\left. + k_1\bar{\sigma} + \frac{k_2}{|x_1| + k^2 e^{-\beta t}} sgn(\bar{\sigma}) + k_3 sgn(\bar{\sigma}) \right]
\end{aligned} \qquad (18)$$

where $k_1 > 0$, $k_2 > c\lambda$, and $k_3 > \lambda + \mu$.

Proof. Taking the derivative of the sliding surface $\bar{\sigma}$ defined in equation (13) yields

$$\dot{\bar{\sigma}} = a(x) + bu + \frac{cke^{-\beta t}\left(x_2 k + kd - 2x_1\dot{k}\right)}{\left(|x_1| + k^2 e^{-\beta t}\right)^2} + \dot{\hat{d}} \qquad (19)$$

Using the control law (18) into (19) leads to

$$\dot{\bar{\sigma}} = -k_1\bar{\sigma} - k_2 sgn(\bar{\sigma}) + \frac{ck^2 e^{-\beta t}\left(d - \hat{d}\right)}{\left(|x_1| + k^2 e^{-\beta t}\right)^2} + \dot{\hat{d}} \qquad (20)$$

The candidate Lyapunov function is as follows

$$V(\bar{\sigma}) = \frac{\bar{\sigma}^2}{2} \qquad (21)$$

Accordingly, the derivative of $V(\bar{\sigma})$ in equation (21) is

$$\begin{aligned}
\dot{V}(\bar{\sigma}) &= -k_1\bar{\sigma}^2 - \frac{k_2}{|x_1| + k^2 e^{-\beta t}}|\bar{\sigma}| - k_3|\bar{\sigma}| \\
&\quad + \frac{ck^2 e^{-\beta t}\left(d - \hat{d}\right)\bar{\sigma}}{\left(|x_1| + k^2 e^{-\beta t}\right)^2} + \dot{\hat{d}}\bar{\sigma}
\end{aligned} \qquad (22)$$

$$\leq -k_1\bar{\sigma}^2 - \frac{k_2 - c|d - \hat{d}|}{|x_1| + k^2 e^{-\beta t}} - \left(k_3 - \left|\dot{\hat{d}}\right|\right)|\bar{\sigma}|$$

Considering that $\|e_d\| \leq \lambda$, and $|\dot{d}| \leq \mu$ in the extended DO, then $|\dot{\hat{d}}| = |\dot{d} - \dot{\hat{d}}| + |\dot{d}| \leq \lambda + \mu$, equation (18) can be rewritten as follows

$$\dot{V}(\bar{\sigma}) \leq -k_1\bar{\sigma}^2 - \frac{k_2 - c\lambda}{|x_1| + k^2 e^{-\beta t}}|\bar{\sigma}| - (k_3 - \lambda - \mu)|\bar{\sigma}| \qquad (23)$$

Considering that $k_1 > 0$, $k_2 > c\lambda$, and $k_3 > \lambda + \mu$, it can be derived from equation (23) that the system will reach the designed sliding surface $\bar{\sigma} = 0$ in finite time according to Lyapunov stability theory.

Remark 4. The sliding mode in the adaptive sliding mode control with extended disturbance observer (EDO-ASMC) method is insensitive to unmatched uncertainties even if the disturbance estimation error of the DO exists.

Numerical example

Example 1

Considering the following illustrative example[5,6]

$$\begin{aligned}
\dot{x}_1 &= x_2 + d(t) \\
\dot{x}_2 &= -2x_1 - x_2 + e^{x_1} + u \\
y &= x_1
\end{aligned} \qquad (24)$$

Constant disturbance. Here, the proposed control method is evaluated using case 2.[5] For this illustration, a constant disturbance $d = 0.5$ is applied at $t = 2$ s and the initial state value is $x(0) = [0, 0]^T$. For comparison studies, four methods including improved nonlinear sliding mode control (INSMC),[29] the DO-SMC,[5] EDO-MSMC[6], and the EDO-ASMC are employed in the control design for system (24). The control parameters of all the four control methods are listed in Table 1.

It can be seen from Figure 1 that the performances are similar for the DO-SMC, EDO-MSMC, and the EDO-ASMC, but DO-SMC and EDO-MSMC have the substantial chattering due to the fact that the switch control is a discontinuous process, while the chattering problem in the proposed EDO-ASMC can be almost eliminated. However, the INSMC method failed to drive the state x_1 to the desired equilibrium, which the INSMC method is sensitive to mismatched disturbance.

Complex disturbance. In this case, the proposed method is evaluated using the complex mismatched disturbance.[6]

The unmatched disturbance can be defined as follows

Table 1. Control parameters for the numerical example case 1.

Controllers	Parameters
INSMC	$F = 5, P = 0.1, k = 1, \beta = 1, k_1 = 0, k_2 = 3$
DO-SMC	$c = 5, \ k = 3, \ l = [6, 0]$
EDO-MSMC	$c = 5, \ k_l = 1, \ k_s = 1.5, \ l_{11} = 50, \ l_{12} = 10$
EDO-ASMC	$c = 1, \ \beta = 2, \ k_1 = 1, \ k_2 = 0.005, \ k_3 = 1, \ l_{11} = 50, \ l_{12} = 10$

INSMC: improved nonlinear sliding mode control; DO-SMC: sliding mode control with disturbance observer; EDO-MSMC: extended disturbance observer–modified sliding mode control; EDO-ASMC: adaptive sliding mode control with extended disturbance observer.
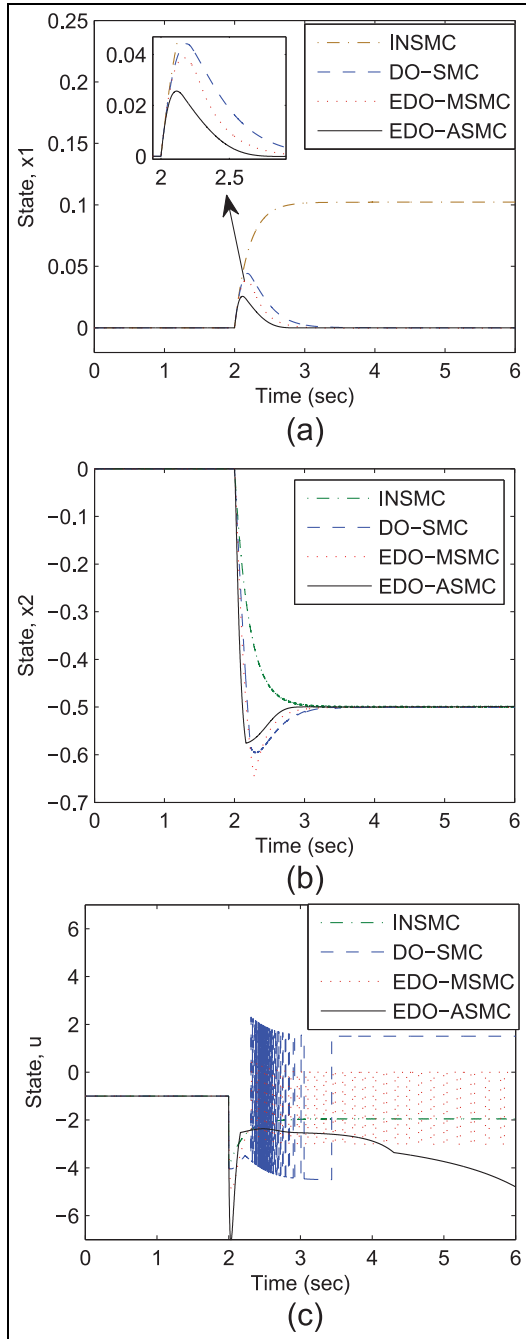
Figure 1. Comparison among INSMC, DO-SMC, EDO-MSMC, and EDO-ASMC: (a) plot of x_1, (b) plot of x_2, and (c) plot of u.

$$d_1(t) = \begin{cases} \dfrac{t}{6} + \sin^2(2t) - \cos(2t) & t < 2 \\ \dfrac{t}{6} + \sin^2(2t) - \cos(2t) + 1 & t \geq 2 \end{cases} \quad (25)$$

and a step change appears after 2 s. The initial state value is set as $x(0) = [1, 0]^T$. The control parameters of all the three control methods are listed in Table 2.

It can be observed from Figure 2(a) that the state x_1 of the proposed control method can rapidly converge to desired equilibrium in the presence of complex mismatched disturbance; on the contrary, the adverse control effects, such as the undesired overshooting, oscillation, and unsatisfactory settling time, appear in the DO-SMC and the EDO-MSMC method. The performances of the state x_2 are similar for the three controls after 2.5 s in Figure 1(b). It is also noticed from Figure 2(c) that the DO-SMC and the EDO-MSMC result in the chattering in the control input response, while the chattering in the EDO-ASMC can be almost eliminated. Moreover, the proposed method is adapted best to the complex disturbance compared with the other two methods and is insensitive to the initial of the complex mismatched disturbance at $t = 2$ s.

Example 2: MAGLEV suspension system

MAGLEV suspension dynamic model. The dynamic model of a MAGLEV suspension system, which is subjected to the mismatched disturbance, is as follows[5]

$$\begin{cases} \dot{x} = Ax + B_u u + B_d d \\ y = Cx \end{cases} \quad (26)$$

where the states are the current, vertical electromagnet velocity, and air gap, that is, $x = [i, \dot{z}, (z_t - z)]$, the input $u = u_{coil}$ is the voltage, and the track input $d = \dot{z}_t$ is the rail vertical velocity. The controlled variable is the variation of air gap, that is, $y = z_t - z$. The detailed modeling produce can be found in the work by Michail.[30] Here, the state matrix A, the input matrix B_u, the disturbance matrix B_d, and the output matrix C are following

Table 2. Control parameters for the numerical example case 2.

Controllers	Parameters
DO-SMC	$c = 5$, $k = 5$, $l = [10, 0]$
EDO-MSMC	$c = 5$, $k_l = 3$, $k_s = 5$, $l_{11} = 50$, $l_{12} = 10$
EDO-ASMC	$c = 5$, $\beta = 2$, $k_1 = 1$, $k_2 = 0.005$, $k_3 = 1$, $l_{11} = 50$, $l_{12} = 10$

DO-SMC: sliding mode control with disturbance observer; EDO-MSMC: extended disturbance observer–modified sliding mode control; EDO-ASMC: adaptive sliding mode control with extended disturbance observer.
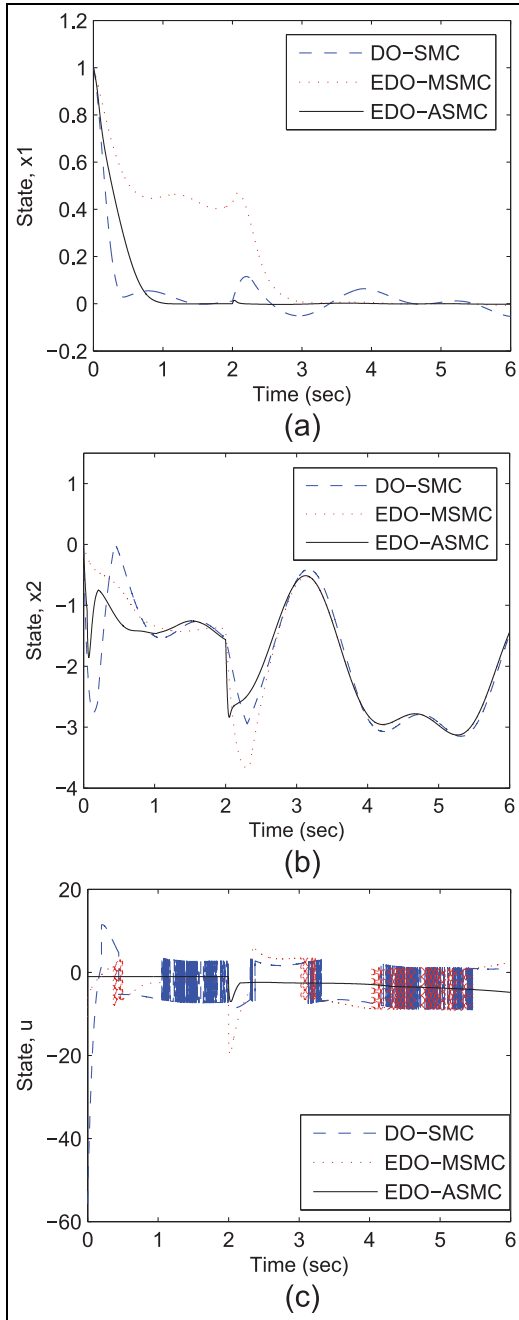
Figure 2. Comparison among DO-SMC, EDO-MSMC, and EDO-ASMC in the presence of complex disturbances: (a) plot of x_1, (b) plot of x_2, and (c) plot of u.

Table 3. Parameters of MAGLEV suspension system.

Parameters	Meaning	Value
M_s	Carriage mass	1000 kg
F_0	Nominal force	9810 N
G_0	Nominal air gap	0.015 m
R_c	Coil's resistance	10 Ω
B_0	Nominal flux density	1 T
L_c	Coil's inductance	0.1 H
I_0	Nominal current	10 A
N_c	Number of turns	2000
V_0	Nominal voltage	1000 V
A_p	Pole face area	0.01 m^2

MAGLEV: MAGnetic LEVitation.

$$A = \begin{bmatrix} \dfrac{-R_c}{L_c + K_b N_c \frac{A_p}{G_0}} & \dfrac{-K_b N_c A_p I_0}{G_0^2 \left(L_c + K_b N_c \frac{A_p}{G_0}\right)} & 0 \\ -2K_f \dfrac{I_0}{M_s G_0^2} & 0 & 2K_f \dfrac{I_0^2}{M_s G_0^3} \\ 0 & -1 & 0 \end{bmatrix} \tag{27}$$

$$B_u = \begin{bmatrix} \dfrac{1}{L_c + K_b N_c \frac{A_p}{G_0}} & 0 & 0 \end{bmatrix}^T \tag{28}$$

$$B_d = \begin{bmatrix} \dfrac{K_b N_c A_p I_0}{G_0^2 \left(L_c + K_b N_c \frac{A_p}{G_0}\right)} & 0 & 1 \end{bmatrix}^T \tag{29}$$

$$C = \begin{bmatrix} 0 & 0 & 1 \end{bmatrix} \tag{30}$$

The physical meanings of the parameters in equations (27)–(30) are listed in Table 3. The major external disturbance in the MAGLEV suspension system comes from deterministic inputs to the suspension in the vertical direction. Such deterministic inputs are the transitions onto the track gradients. Deterministic input components considered here are referred Michail[30] and shown in Figure 3. They represent a gradient of 5% at a vehicle speed of 15 m/s, while the jerk level is 1 m/s^3. The control specifications of the MAGLEV system under consideration of the deterministic track input are given in Table 4.

Control design. In order to implement the proposed method for the MAGLEV system, the following coordinate transformation is introduced
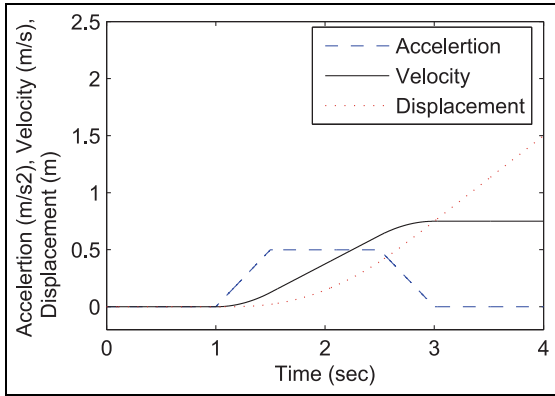
Figure 3. Track input to the suspension with a vehicle speed of 15 m/s and 5% gradient.

Table 4. Constraints for MAGLEV suspension system.

Constraints	Value
Maximum air gap deviation $((z_t - z)_p)$	$\leqslant 0.0075$ m
Maximum input coil voltage $((u_{coil})_p)$	$\leqslant 300\,V(3l_0R_c)$
Settling time (t_s)	$\leqslant 3$ s
Air gap steady-state error $((z_t - z)_{ess})$	0

MAGLEV: MAGnetic LEVitation.

$$\xi = Px \qquad (31)$$

where $P = \begin{bmatrix} C & CA & CA^2 \end{bmatrix}^T$.

Using this coordinate transformation, the MAGLEV system can be rewritten as follows

$$\dot{\xi} = \overline{A}\xi + \overline{B}_u u + \overline{B}_d d \qquad (32)$$

where $\overline{A} = PAP^{-1}$, $\overline{B}_u = PB_u$, and $\overline{B}_d = PB_d$. Using the parameters in Table 3 into equation (32) leads to

$$\begin{cases} \dot{\xi}_1 = \xi_2 + d \\ \dot{\xi}_2 = \xi_3 \\ \dot{\xi}_3 = CA^3P^{-1}\xi + CA^2B_u u + CA^2B_d d \end{cases} \qquad (33)$$

The following extended DO (9) is employed to estimate the disturbance in the MAGLEV system.

In order to use the proposed method for high-order system (33), the backstepping method is also applied to design the control law.

First, the proposed method is used for the states ξ_1 and ξ_2 in system (33), and the sliding mode $\sigma_\xi = \xi_2 + (c\xi_1/(|\xi_1| + k^2e^{-\beta t})) + \hat{d}$, where $c > \lambda$, $k_1 > 0$, $k_2 > c\lambda$, and $k_3 > \lambda + \mu$, can be obtained.

Second, the virtual control ξ_{3v} using the proposed method is chosen as follows

$$\xi_{3v} = -\frac{cke^{-\beta t}\left(k\xi_2 - k\hat{d} - 2\xi_1\dot{k} + \xi_1 k\beta\right)}{(|\xi_1| + k^2e^{-\beta t})^2} - k_1\sigma_\xi - k_2 sgn(\sigma_\xi) \qquad (34)$$

Let $e_3 = \xi_3 - \xi_{3v}$, the EDO-ASMC law for the MAGLEV suspension system is as follows

$$u = -\left(CA^2B_u\right)^{-1} \\ \left[CA^3P^{-1}\xi + CA^2B_d\hat{d} - \dot{\xi}_{3v} + k_{1e}e_3 + k_{2e}sgn(e_3)\right] \qquad (35)$$

where $k_{1e} > 0$ and $k_{2e} > CA^2B_d|\hat{d} - d|$.

Simulation results. In order to evaluate the performance of the proposed method, the proposed method is compared with the DO-SMC and the EDO-MSMC. The sliding surface of the DO-SMC method for the MAGLEV suspension system is designed as follows

$$\sigma_1 = c_1\xi_1 + c_2\left(\xi_2 + \hat{d}\right) + c_3\xi_3 \qquad (36)$$

where the parameter $c_i(i = 1, 2, 3)$ satisfies the Hurwitz polynomial $c_3s^2 + c_2s + c_1 = 0$. Then, DO can be obtained as follows

$$\begin{cases} \dot{p} = -L\overline{B}_d(p + L\xi) - L\left(\overline{A}\xi + \overline{B}_u u\right) \\ \hat{d} = p + L\xi \end{cases} \qquad (37)$$

where $\hat{d}$ is the disturbance estimate, p is an auxiliary vector, and L is the observer gain matrix to be designed. Accordingly, the corresponding DO-SMC law is as follows

$$u = -\left(CA^2B_u\right)^{-1} \\ \left\{CA^3P^{-1}\xi + CA^2B_d\hat{d} + c_3^{-1}\left[k_\sigma sgn(\sigma_1) + c_1\left(\xi_2 + \hat{d}\right) + c_2\xi_3\right]\right\} \qquad (38)$$

The sliding surface of the EDO-MSMC method for the MAGLEV suspension system is designed as follows

$$\sigma_2 = \sigma_{21} + \sigma_{21}(0)e^{-\alpha t} \qquad (39)$$

where $\sigma_{21} = \overline{c}_1\xi_1 + \overline{c}_2(\xi_2 + \hat{d}) + \overline{c}_3\xi_3 + \hat{d}_1$, d_1 and $\hat{d}_1$ are estimates of d and $\dot{d}$, respectively, and the parameter $c_i(i = 1, 2, 3)$ also satisfies the Hurwitz polynomial $\overline{c}_3s^2 + \overline{c}_2s + \overline{c}_1 = 0$.

The EDO can be obtained as follows

$$\begin{cases} \hat{d}_1^{j-1} = p_{1j} + l_{1j}\xi_1 \\ \dot{p}_{1j} = -l_{1j}\left(\xi_2 + \hat{d}_1\right) + \hat{d}_1^j \\ \dot{p}_{13} = -l_{13}\left(\xi_2 + \hat{d}_1\right) \end{cases} \qquad (40)$$

where p_{1j} is the auxiliary variable, $j = 1, 2$, and l_{1r} is the observer gain matrix to be designed, $r = 1, 2, 3$.

Accordingly, the corresponding EDO-MSMC law is as follows

Table 5. Control parameters for the MAGLEV suspension in case 1.

Controllers	Parameters
DO-SMC	$c_1 = 100,\ c_2 = 20,\ c_3 = 1,\ k = 60,\ l = [100, 0, 0]$
EDO-MSMC	$\bar{c}_1 = 100,\ \bar{c}_2 = 20,\ \bar{c}_3 = 1,\ k_l = 10,\ k_s = 30,\ l_{11} = 50,\ l_{12} = 10,\ l_{13} = 10$
EDO-ASMC	$c = 2,\ \beta = 2,\ k_1 = 1,\ k_2 = 0.01,\ k_3 = 2,\ k_{1e} = 1,\ k_{2e} = 2,\ l_{11} = 50,\ l_{12} = 10,\ l_{13} = 10$

MAGLEV: MAGnetic LEVitation; DO-SMC: sliding mode control with disturbance observer; EDO-MSMC: extended disturbance observer–modified sliding mode control; EDO-ASMC: adaptive sliding mode control with extended disturbance observer.
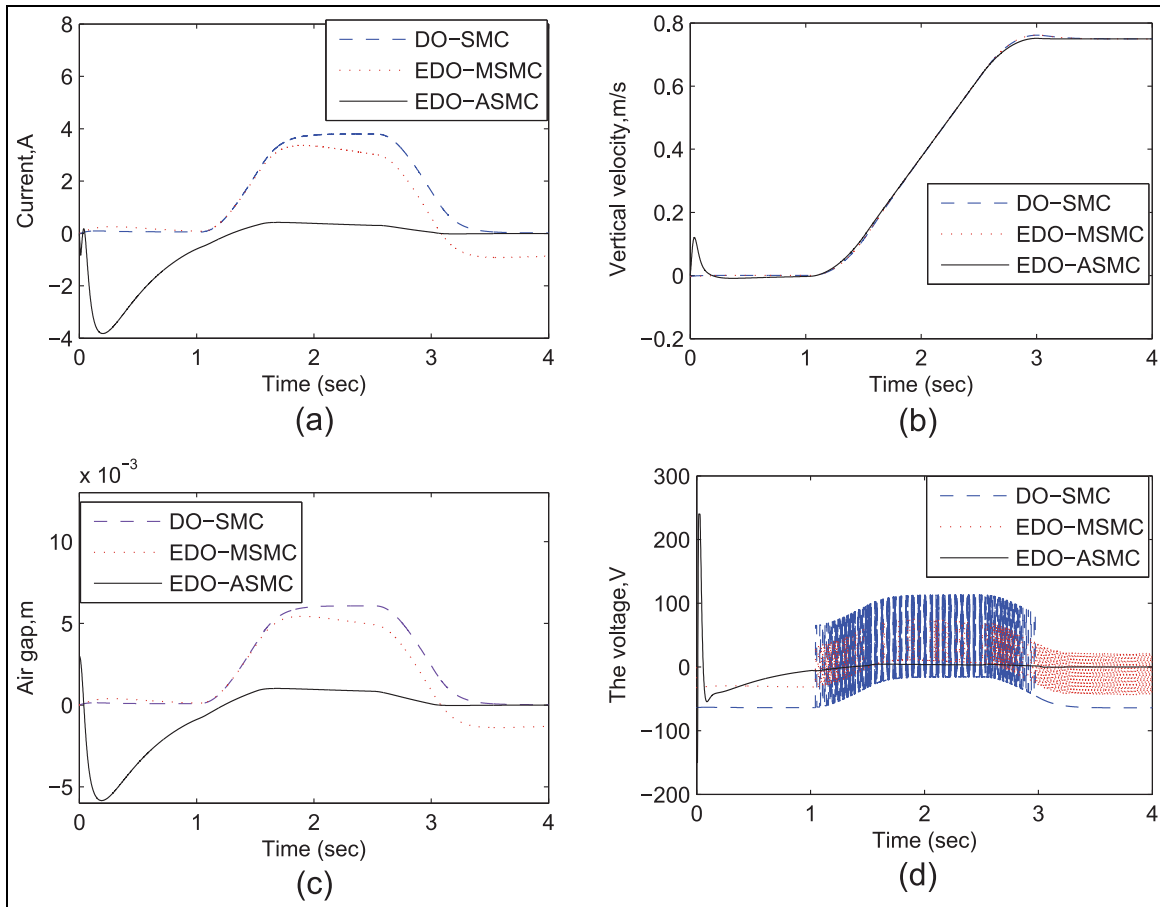
Figure 4. Comparison among DO-SMC, EDO-MSMC, and EDO-ASMC in the MAGLEV suspension system: (a) plot of the current i, (b) plot of vertical velocity $\dot{z}$, (c) plot of the air gap $\dot{z} - z$, and (d) plot of the voltage of the coil u_{coil}.

$$u = -\left(CA^2 B_u\right)^{-1}\left\{ CA^3 P^{-1}\xi + CA^2 B_d \hat{d}_1 + \bar{c}_3^{-1}\left[\alpha\sigma_{21}(0)e^{-\alpha t} + k_l\sigma_2 + k_s sgn(\sigma_2) + \bar{c}_1\left(\xi_2 + \hat{d}_1\right) + \bar{c}_2\left(\xi_3 + \hat{d}_1\right)\right] + \dot{\hat{d}}_1\right\} \quad (41)$$

The initial state values of MAGLEV suspension system (26) are set as $\begin{bmatrix} i(0) & \dot{z}(0) & (z_t - z)(0) \end{bmatrix}^T = \begin{bmatrix} 0 & 0 & 0.03 \end{bmatrix}^T$. The external disturbance, as displayed in Figure 3, is imposed on the system. For comparison studies, the DO-SMC and EDO-MSMC are also employed in the MAGLEV suspension system. The parameters of three control methods are listed in Table 5. Response curves of the states and inputs of the MAGLEV system are shown in Figure 4. When the

system suffers from the mismatched disturbance, the proposed EDO-ASMC obtains better disturbance rejection performance than DO-SMC and EDO-MSMC. The chattering in the sliding mode has been almost eliminated in the EDO-ASMC, while the chattering still exists in the sliding mode of the DO-SMC and the EDO-MSMC.

The other deterministic input components, as shown in Figure 5, are considered. They represent the jerk level

Table 6. Control parameters for the MAGLEV suspension in case 2.

| Controllers	Parameters
DO-SMC	$c_1 = 100$, $c_2 = 20$, $c_3 = 1$, $k = 60$, $l = [100, 0, 0]$
EDO-MSMC	$\bar{c}_1 = 100$, $\bar{c}_2 = 20$, $\bar{c}_3 = 1$, $k_l = 10$, $k_s = 20$, $l_{11} = 50$, $l_{12} = 10$, $l_{13} = 10$
EDO-ASMC	$c = 2$, $\beta = 2$, $k_1 = 0$, $k_2 = 0.01$, $k_3 = 2$, $k_{1e} = 1$, $k_{2e} = 2$, $l_{11} = 50$, $l_{12} = 10$

MAGLEV: MAGnetic LEVitation; DO-SMC: sliding mode control with disturbance observer; EDO-MSMC: extended disturbance observer–modified sliding mode control; EDO-ASMC: adaptive sliding mode control with extended disturbance observer.
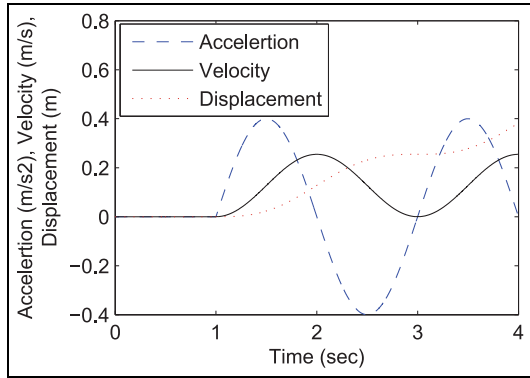
Figure 5. Track input to the suspension with a jerk level with sine wave.

which is sine wave with magnitude of $0.4 \, \text{m/s}^3$. The control parameters of three control methods are listed in Table 6.

The response curves of the states and inputs in this case are shown in Figure 6. By comparing with the first simulation scenario, it can be observed from Figure 6 that the states of the MAGLEV system for the proposed EDO-ASMC have hardly affected by the mismatched disturbance with time variation, while the states of the system for the DO-SMC and the EDO-MSMC are severely affected by the mismatched disturbance. Moreover, with respect to the DO-SMC and the EDO-MSMC, the chattering in the sliding mode of the proposed EDO-ASMC is significantly eliminated.
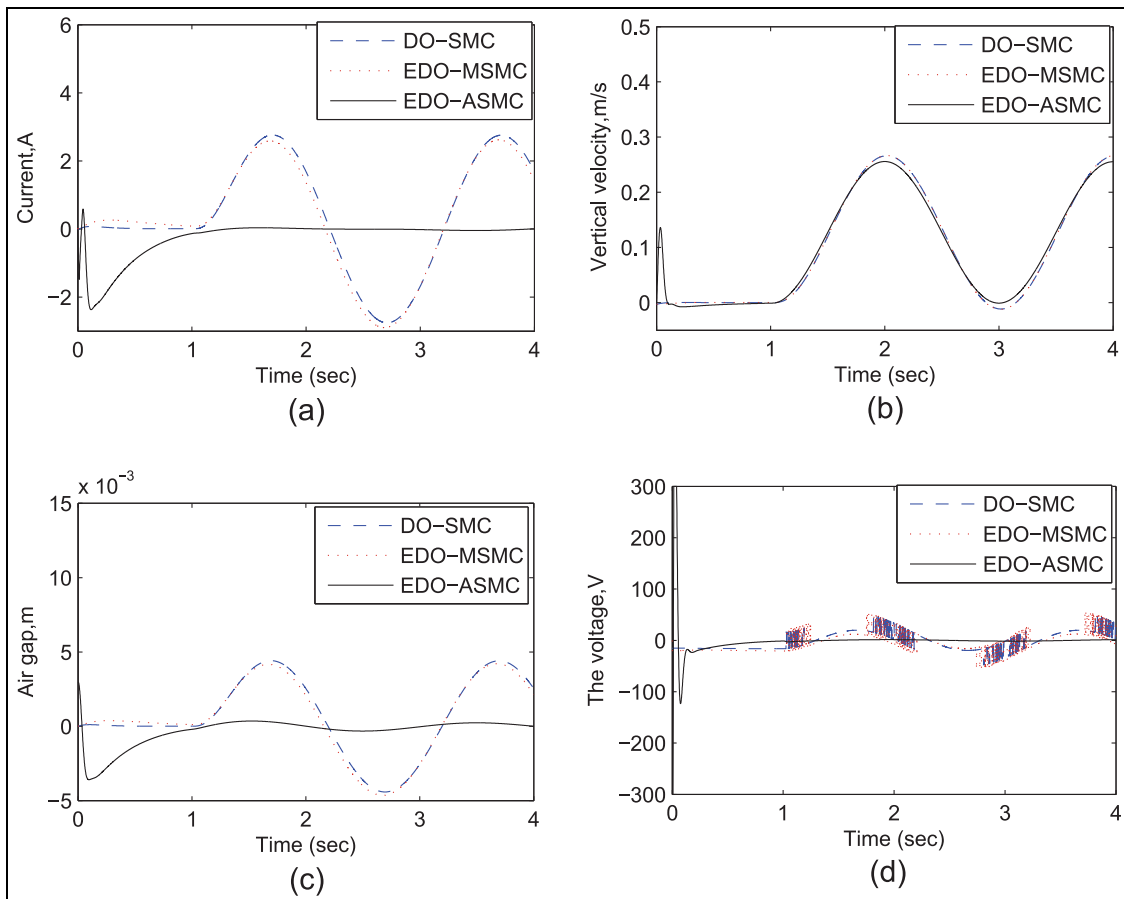
Figure 6. Comparison among DO-SMC, EDO-MSMC, and EDO-ASMC in the MAGLEV suspension system: (a) plot of the current i, (b) plot of vertical velocity $\dot{z}$, (c) plot of the air gap $\dot{z} - z$, and (d) plot of the voltage of the coil u_{coil}.

Conclusion

In this article, a new disturbance attenuation–based SMC approach has been proposed to reduce the effect of mismatched uncertainties on the control system. A new adaptive sliding mode surface, in which the disturbance estimation is designed according to the sliding motion along the sliding surface, is proposed for driving the states to the desired equilibrium point in the presence of mismatched uncertainties. Both numerical and application examples have been simulated to demonstrate the effectiveness as well as the superiorities of the proposed method. The results have shown that the proposed method exhibits the excellent properties of dynamical performance and chattering reduction compared with other nonlinear SMC methods. Further research will focus on extending the proposed approach to high-order systems.

Declaration of conflicting interests

Funding

References

1. Utkin V. Variable structure systems with sliding modes. *IEEE T Ind Electron* 1977; 22: 212–222.
2. Yu X and Kaynak O. Sliding-mode control with soft computing: a survey. *IEEE T Ind Electron* 2009; 56: 3275–3285.
3. Liu H and Li S. Speed control for PMSM servo system using predictive functional control and extended state observer. *IEEE T Ind Electron* 2012; 59: 1171–1183.
4. Errouissi R, Ouhrouche M, Chen WH, et al. Robust nonlinear predictive controller for permanent-magnet synchronous motors with an optimized cost function. *IEEE T Ind Electron* 2012; 59: 2849–2858.
5. Yang J, Li S and Yu X. Sliding-mode control for systems with mismatched uncertainties via a disturbance observer. *IEEE T Ind Electron* 2013; 60: 160–169.
6. Ginoya D, Shendge PD and Phadke SB. Sliding mode control for mismatched uncertain systems using an extended disturbance observer. *IEEE T Ind Electron* 2014; 61: 1983–1992.
7. Chen WH. Nonlinear disturbance observer-enhanced dynamic inversion control of missiles. *J Guid Control Dynam* 2003; 26: 161–166.
8. Chwa D, Choi JY and Anavatti SG. Observer-based adaptive guidance law considering target uncertainties and control loop dynamics. *IEEE T Contr Syst T* 2006; 14: 112–123.
9. Choi HH. LMI-based sliding surface design for integral sliding mode control of mismatched uncertain systems. *IEEE T Automat Contr* 2007; 52: 736–742.
10. Kim KS, Park Y and Oh SH. Designing robust sliding hyperplanes for parametric uncertain systems: a Riccati approach. *Automatica* 2000; 36: 1041–1048.
11. Tao CW, Chan ML and Lee TT. Adaptive fuzzy sliding mode controller for linear systems with mismatched time-varying uncertainties. *IEEE T Syst Man Cy B* 2003; 33(2): 283–294.
12. Wang SW, Yu DW and Yu DL. Compensation for unmatched uncertainty with adaptive RBF network. *Int J Eng Sci Technol* 2011; 18: 801–804.
13. Wang C, Hou Y, Gao Q, et al. Electric load simulator system control based on adaptive particle swarm optimization wavelet neural network with double sliding modes. *Adv Mech Eng* 2016; 8: 1–10.
14. Jiao X and Jiang J. Design of adaptive switching control for hypersonic aircraft. *Adv Mech Eng* 2015; 7: 1–10.
15. Sagliano M, Mooij E and Theil S. Adaptive disturbance-based high-order sliding-mode control for hypersonic-entry vehicles. *J Guid Control Dynam* 2016; 40: 521–532.
16. Weng Y and Gao X. Adaptive sliding mode decoupling control with data-driven sliding surface for unknown MIMO nonlinear discrete systems. *Circ Syst Signal Pr* 2017; 36: 969–997.
17. Matthews GP and Decarlo RA. Decentralized tracking for a class of interconnected nonlinear systems using variable structure control. *Automatica* 1988; 24: 187–193.
18. Polyakov A and Poznyak A. Invariant ellipsoid method for minimization of unmatched disturbances effects in sliding mode control. *Automatica* 2011; 47: 1450–1454.
19. Liang YW, Ting LW and Lin LG. Study of reliable control via an integral-type sliding mode control scheme. *IEEE T Ind Electron* 2012; 59: 3062–3068.
20. Dong B and Li Y. Decentralized integral nested sliding mode control for time varying constrained modular and reconfigurable robot. *Adv Mech Eng* 2015; 7: 317127.
21. Elhajji Z, Dehri K and Nouri AS. Stability analysis of discrete integral sliding mode control for input-output model. *J Dyn Syst: T ASME* 2016; 139: 034501.
22. Sam YM, Osman JHS and Ghani MRA. A class of proportional-integral sliding mode control with application to active suspension system. *Syst Control Lett* 2004; 51: 217–223.
23. Errouissi R and Ouhrouche M. Nonlinear predictive controller for a permanent magnet synchronous motor drive. *Math Comput Simulat* 2010; 81: 394–406.
24. Estrada A and Fridman LM. Integral HOSM semiglobal controller for finite-time exact compensation of unmatched perturbations. *IEEE T Automat Contr* 2010; 55: 2645–2649.
25. Zheng X, Li P, Li H, et al. Adaptive backstepping-based NTSM control for unmatched uncertain nonlinear systems. *J Syst Eng Electron* 2015; 26: 557–564.
26. Yang J, Li S, Su J, et al. Continuous nonsingular terminal sliding mode control for systems with mismatched disturbances. *Automatica* 2013; 49: 2287–2291.
27. Kolsi-Gdoura E, Feki M and Derbel N. Observer based robust position control of a hydraulic servo system using

variable structure control. *Math Probl Eng* 2015; 2015: 1–11.

28. Qian DW, Tong SW and Li CD. Observer-based leader-following formation control of uncertain multiple agents by integral sliding mode. *Bull Pol Acad Sci: Te* 2017; 65: 35–44.

29. Qian R, Luo M and Sun P. Improved nonlinear sliding mode control based on load disturbance observer for permanent magnet synchronous motor servo system. *Adv Mech Eng* 2016; 8: 1–12.

30. Michail K. *Optimised configuration of sensing elements for control and fault tolerance applied to an electromagnetic suspension system*. PhD Thesis, Loughborough University, Loughborough, 2014.